AFRL-ML-TY-TP-2007-4538

POSTPRINT

RESISTANCE OF MEMBRANE RETROFIT CONCRETE MASONRY WALLS TO LATERAL PRESSURE

Lee G. Moradi, James S. Davidson

Applied Research Associates
P.O. Box 40128
Tyndall AFB, FL 32403-5323

Robert J. Dinan, Ph.D.
Air Force Research Laboratory

APRIL 2008

AIRBASE TECHNOLOGIES DIVISION
MATERIALS AND MANUFACTURING DIRECTORATE
AIR FORCE RESEARCH LABORATORY
AIR FORCE MATERIEL COMMAND
139 BARNES DRIVE, SUITE 2
TYNDALL AIR FORCE BASE, FL 32403-5323

REPORT DOCUMENTATION PAGE

1. REPORT DATE *(DD-MM-YYYY)*	2. REPORT TYPE	3. DATES COVERED *(From - To)*

4. TITLE AND SUBTITLE	5a. CONTRACT NUMBER
	5b. GRANT NUMBER
	5c. PROGRAM ELEMENT NUMBER
6. AUTHOR(S)	5d. PROJECT NUMBER
	5e. TASK NUMBER
	5f. WORK UNIT NUMBER

7. PERFORMING ORGANIZATION NAME(S) AND ADDRESS(ES)	8. PERFORMING ORGANIZATION REPORT NUMBER

9. SPONSORING/MONITORING AGENCY NAME(S) AND ADDRESS(ES)	10. SPONSOR/MONITOR'S ACRONYM(S)
	11. SPONSOR/MONITOR'S REPORT NUMBER(S)

12. DISTRIBUTION/AVAILABILITY STATEMENT

13. SUPPLEMENTARY NOTES

14. ABSTRACT

15. SUBJECT TERMS

16. SECURITY CLASSIFICATION OF:			17. LIMITATION OF ABSTRACT	18. NUMBER OF PAGES	19a. NAME OF RESPONSIBLE PERSON
a. REPORT	b. ABSTRACT	c. THIS PAGE			
					19b. TELEPHONE NUMBER *(Include area code)*

Resistance of Membrane Retrofit Concrete Masonry Walls to Lateral Pressure

Lee G. Moradi, PE[1]; James S. Davidson[2]; Robert J. Dinan[3]

ABSTRACT

This paper first describes the current state of analysis for the response of unreinforced concrete masonry walls subjected to lateral uniform pressure. The formulation is based on the initial elastic response, the subsequent initiation of cracks and the nonlinear rocking response, and the eventual large displacement and wall's potential collapse. The necessary equations are developed for these phases in the form of a resistance function. The paper then incorporates membrane retrofit materials to strengthen the wall's resistance to lateral pressure, and develops the necessary resistance function equations. In blast tests, membrane retrofit unreinforced masonry walls have experienced severe cracking and large displacements without collapse. This is of high interest to the areas of DOD Force Protection, the Department of Homeland Security, and the construction industry impacted by hurricanes and other high wind events. The paper concludes with several illustrations and examples that the application of membrane retrofits indeed increases the resistance of the wall to lateral pressure.

CE Database Subject Headings: Walls, Masonry, Retrofit, Blast, Protection, Resistance

[1]Director of Engineering, Center for Biophysical Sciences and Engineering, The University of Alabama at Birmingham, CBSE 100, 1530 Third Avenue South, Birmingham, AL, 35294. T (205) 975-2718, F (205)-975-1709, Email: moradi@uab.edu
[2]Associate Professor, Department of Civil & Environmental Engineering, the University of Alabama at Birmingham, AL 35294
[3]Senior Research Engineer, Air Force Research Laboratory, 139 Barnes Dr., Suite 2, Tyndall AFB, FL 32403

BACKGROUND AND INTRODUCTION

The largely empirical design of masonry structures does not "rely extensively on the rational application of engineering principles," which can result in the designer not fully recognizing all of the relevant design variables (Yokel and Dikkers 1971). Design variables such as loading geometry, end fixity, wall stiffness, and cross-sectional properties can have significant effects on the overall strength of masonry walls. In 1971, Yokel and Dikkers reported a study on the strength of load bearing masonry walls based on 192 full-scale masonry wall tests previously conducted by the National Bureau of Standards and the Structural Clay Products Institute. This study used rational analysis methods, which were based upon established theory, to predict the strength of load bearing masonry walls (Yokel and Dikkers 1971). In the same year, Yokel developed a methodology for stability and load capacity of members with no tensile strength (Yokel 1971). Eccentrically loaded compression members were examined beginning with their elastic behavior through the cracked and rocking rigid body behavior until ultimate load capacity was reached. Yokel developed equations for strength calculations of such compression members and verified his results with 39 full-scale tests on brick walls.

Extensive seismic studies were performed as part of a broad investigation aimed at developing standards for the renovation of unreinforced masonry buildings in Los Angeles, particularly with respect to acceptance height to thickness ratio of walls (ABK 1981, Kariotis 1986). The study investigated the one-way behavior of eight wall specimens of varying construction and geometry under a range of gravity loads and several dynamic motions at top and bottom, simulating the input seismic motion from the ground or from a diaphragm anchorage. The study concluded that the primary concern is

2

"dynamic stability" - - the equilibrium of the cracked wall under the influence of applied loads, self weight, and inertial loads rather than material stress levels. The results showed close correlation with the tests and were presented in an eight-volume report produced by ABK. In 1985, Priestley developed a similar methodology to examine the behavior of one-way unreinforced masonry walls under the action of lateral seismic loads (Priestley 1985). The methodology was later corrected in 1986 (Priestley 1986) with a final publication in 1992 (Paulay et al. 1992). It suggested that the formation of cracks did not constitute wall failure, even in unreinforced masonry walls. Failure occurs only when the resultant compression force from surcharge and wall weight above the crack is displaced outside the line of action of the applied gravity loads at the top and bottom of the wall (Paulay et al. 1992). The method determines the nonlinear load-deflection curve for a masonry wall subjected to out-of-plane loading.

In 1995, La Mendola et al. examined stability conditions of masonry walls subjected to seismic transverse forces. The problem was translated into the analysis of a fixed-free ended prismatic column undergoing static horizontal forces equivalent to maximum inertia actions. Hamid et al. (1988) investigated fracture of masonry structures using the finite element approach. This investigation resulted in constitutive models capable of simulating the initiation and propagation of fracture under combined normal and shear stresses in both tension-shear and compression-shear regions. The models predicted load carrying capacity of masonry assemblages and provided detailed information on the failure mode, ductility, and crack patterns. Drysdale et al. (1994) used a very similar approach to that employed by Yokel (1971) and Priestley (1986) to develop a resistance function for unreinforced masonry walls under lateral loads. The approach considered

3

arching for one-way action walls confined between rigid boundaries at their top and bottom interfaces. The results showed significant increase in the resistance of such walls to lateral loads. Martini (1997) investigated one-way and two-way action of unreinforced masonry walls using the finite element method and showed excellent correlation with the approach proposed by Fattal (1976), Priestley (1986), Paulay et al. (1992) and La Mendola (1995).

The earliest in-depth investigation of the arching action theory of unreinforced masonry walls was carried out by McDowell et al. (1956). It represented a rather radical departure from the resistance of lateral forces usually assumed for this type of construction. The theory was used to obtain the static load-deflection curves for masonry beams of solid cross section. The results showed significant improvement in the resistance of these beams to lateral uniform loads.

McDowell et al. (1956) noted that under certain conditions masonry walls withstood much larger loads than those predicted on the basis of conventional bending analysis. The additional strength was developed when the walls were butted up against supports which were essentially rigid. These type of walls exhibited three to six times the load-carrying capacity of simply supported walls. A series of static tests were performed on different sizes of solid unreinforced masonry beams exposed to lateral uniform loads, and the results were documented as compared to those derived from their proposed theory.

Gabrielsen et al. (1973 and 1975) performed extensive blast tests on unreinforced masonry walls with arching action. Shock tunnel pressure waves were used to simulate the level of blast load required for each test. The tests showed that walls with arching action are considerably stronger, by as much as four to five times, than walls without.

4

Walls with gaps and arching action were also shock tunnel tested and the results showed that they were significantly weaker than the walls with arching action and no gaps.

Drysdale et al. (1994) used the same approach as that employed by McDowell et al. (1956) to develop a simpler equation for arching resistance of unreinforced masonry walls under lateral loads. The approach considered arching for one-way action walls confined between rigid boundaries at their top and bottom interfaces. Dinan et. al (2003) examined arching resistance of polymer retrofit concrete masonry walls using the method outlined by Drysdale et. al, and the Wall Analysis Code (WAC) to arrive at resistance functions that matched well with full-scale test data.

The use of polymer retrofits for concrete masonry walls started in the seismic design community. The early in-depth studies arose as part of an investigation into the renovation of unreinforced masonry buildings in Los Angeles (Martini 1996). In earthquake regions, typical unreinforced masonry walls lacked the strength and ductility to survive seismic loads. Carbon overlays were investigated as a repair and retrofit technique for masonry walls during tests of single-story masonry walls (Laursen et al. 1995). The carbon overlays were used in an attempt to enhance shear and flexural strength. The test results indicated "significant strength and deformation capacities increases".

In 1999, researchers at the Air Force Research Laboratory began looking for retrofit techniques to increase the blast resistance of common exterior walls. One of the goals of the research was to develop a retrofit technique that did not have difficult application processes and the high expense of commonly used methods for strengthening walls, such as increasing the mass with reinforced concrete. The need arose for a "lighter weight

solution" that would "introduce ductility and resilience into building walls" (Knox et al. 2000 and ETL 02-4). An elastomeric polymer, with a polyurea base, was chosen for use as a retrofit material based upon the results of material testing performed at Tyndall Air Force Base. The material was selected based on "its strength, flammability, and cost". The application method for this material was a relatively straightforward spray-on process. Full-scale tests were performed using blast-loaded masonry walls and lightweight structures retrofitted with the polymer material. The material was easily sprayed onto the interior and exterior wall surfaces while maintaining control over the application thickness. The full-scale tests showed that the masonry and the lightweight structure walls experienced large deflections without breaching, and that no debris entered the interior of the test structures. The lightweight structure used in the full-scale tests stayed intact, but the structure experienced severe ceiling crushing which needed to be mitigated (Davidson et. al. 2004 and 2005).

PURPOSE

The improved performance of membrane retrofit concrete masonry walls during seismic and blast events are important to public safety. Blast loads caused accidentally or intentionally and high wind conditions during severe thunderstorms, hurricanes, and tornadoes commonly cause catastrophic failures to light weight military, industrial, commercial, and residential building that incorporate unreinforced concrete masonry walls in their construction. Membrane retrofitting of these walls will greatly improve their capacity and the survivability of these buildings. The effort presented herein

provides the formulation to calculate the capacity of membrane retrofit concrete masonry walls for lateral pressure loads.

RESISTANCE FUNCTION DEVELOPMENT

Unreinforced Concrete Masonry Wall

Approach

Unreinforced masonry walls laterally supported along their top and bottom edges resist lateral forces by spanning vertically between these supports (Drysdale et al. 1994). Flexural stresses normal to the bed joints eventually result in tensile failure when a crack occurs along a course of the bed joint. The failure mechanism can be very complex and depends upon the type of supports provided at the top and bottom edges, and the magnitude of axial forces from self weight and any superimposed loads.

In general, the weight of the wall produces a uniform compressive stress throughout the wall. Initially, any tensile stresses developing from bending of the wall due to lateral loads will be suppressed by the compressive stresses due to the weight of the wall. As the lateral forces increase, the impact of compressive stresses decrease on the tension face of the wall, and eventually tensile stresses begin to develop. Because the flexural strength of the mortar joints is quite variable and depends on the construction techniques and weather, it is possible that cracks will initiate at the early stages of tensile stresses. Therefore, it is conservatively assumed in the development of the resistance function that unreinforced masonry walls cannot resist tensile stresses.

Once tensile stresses develop on the tension side of the wall, cracks will initiate along two or three units in the course (Fig. 1) and then immediately propagate for the full

length of the wall (Baker 1977 and 1980). The formation of cracks does not constitute wall failure, even in an unreinforced masonry wall (Priestley and Paulay 1992). The resultant compressive force R in the compression zone of the central crack counteracts the vertical loads due to wall weight and surcharge, and creates a balancing moment against lateral loads (Fig. 2). Increase in lateral loads will result in an increase in compressive stresses that cause R, and subsequently the wall resistance. The increase in compressive stresses and the triangular distribution of these stresses cause R to move towards the compression face of the wall. A maximum compressive stress block will develop in the compression side of the wall that equals the masonry compressive strength. The wall collapses when R moves outside of the line of action of vertical loads, namely wall weight and surcharge.

Analytical Model

In developing the equations to predict conditions for wall failure, the following assumptions and limitations are made.

1. The wall is load-bearing

2. The wall experiences one-way bending action

3. If it is built from hollow concrete masonry, the cells are un-grouted

4. The wall is not reinforced with steel bars

5. Tensile strength of concrete masonry and mortar joints is ignored

6. The lateral load on the wall is constant over the wall height (h)

7. The wall is partially fixed at top and bottom interfaces

The last assumption is made to help develop the necessary equations for wall failure with varying degrees of end fixity. Although most unreinforced concrete masonry walls are simply supported at the top and bottom supports, the ability to specify end fixity makes it convenient when a specific wall design develops moment capacity at the top and bottom supports. The design engineer can determine the degree at which the top and bottom supports develop moment in the wall, and determine the percent end fixity for the analysis. The designer can also be conservative and assume simply supported conditions at the top and bottom supports.

It will be shown that, as long as the end fixity is below 75%, the maximum moment occurs at the mid-height of the wall, and the derivations will stand. The equations will include options to vary the degree of end fixity (α) from 75% to 0% (simply supported).

Consider the wall in Fig. 3, partially fixed end conditions at top and bottom, and lateral pressure p. Summing moments about the base of the wall result in:

$$\circlearrowleft + \sum M_{base} = 0 = Hh - \frac{ph^2}{2} - \frac{w_i \Delta}{2} \tag{1}$$

$$H = \frac{ph}{2} + \frac{w_i \Delta}{2h} \tag{2}$$

Summing moments about point "O" for the upper half of the wall results in:

$$\circlearrowleft + \sum Mo = 0 = -\frac{ph^2}{8} + \frac{w_i \Delta}{4} + \left(\frac{ph}{2} + \frac{w_i \Delta}{2h}\right)\frac{h}{2} - \frac{\alpha ph^2}{12} + P\Delta - Rx \tag{3}$$

$$\Delta = \frac{Rx}{\frac{w_i}{2} + P} - \frac{(3 - 2\alpha)ph^2}{12w_i + 24P} \tag{4}$$

$$R = \frac{w_i}{2} + P \tag{5}$$

9

To address the percentage of end fixity, take the current case where the end moments are equal to $\alpha ph^2/12$. The total combined moments within a uniformly loaded beam is:

$$M_{Total} = M_{end} + M_{middle} = ph^2/8 \tag{6}$$

100% fixed end beams: $M_{end} = ph^2/12$ and $M_{middle} = ph^2/24$ ➡ $M_{total} = ph^2/8$

0% fixed end (S.S.) beams: $M_{end} = 0$ and $M_{middle} = ph^2/8$ ➡ $M_{total} = ph^2/8$

Partially fixed end beams: $M_{end} = \alpha ph^2/12$ and $M_{middle} = (3-2\alpha) ph^2/24$ ➡

$M_{total} = ph^2/8$

For the moment at mid-point to be greater than the moment at the two ends, α must be less than 75%.

Since it is assumed that masonry cannot develop tensile stresses, once the compressive stresses caused by gravity and surcharge are overcome, stresses in the masonry are distributed in a triangular form Fig. 4. R is the resultant force on this triangular stress distribution. As the lateral load increases and the crack in masonry grows, the triangular stress distribution increases in intensity but decreases in length, hence R moves towards the compression face of the wall. This process continues until a compression block is developed very near the compression face of the wall with a stress intensity equal to the strength of masonry. Failure occurs when R moves outside of the line of action of self weight and surcharge.

It can be shown from Fig. 4(c) that:

If: y = length of crack x = distance from "R" to wall centerline

$$x = \frac{t}{2} - \frac{t-y}{3} \tag{7}$$

$$x = \frac{t+2y}{6} \tag{8}$$

Substituting Eqs. 5 and 8 into Eq. 4 results in a relationship for wall displacement versus lateral load:

$$\Delta = \frac{t}{6} + \frac{y}{3} - \frac{(3 - 2\alpha)ph^2}{12w_i + 24P}$$ (9)

Which yields:

$$\Delta = \frac{t}{6} + \frac{y}{3} - \frac{ph^2}{4w_i + 8P}$$ for $\alpha = 0\%$ Simply supported ends (10)

$$\Delta = \frac{t}{6} + \frac{y}{3} - \frac{ph^2}{6w_i + 12P}$$ for $\alpha = 50\%$ Partially fixed ends (11)

Elastic deflection of the wall prior to crack is calculated using Eq. 13 below. This equation accounts for variation in end fixity of the wall and is derived using simple elastic beam theory with uniformly distributed load and equal end moments (M_e):

$$\Delta_{max.elastic} = \frac{ph}{48EI}\left(\frac{5h^3}{8} - \frac{6M_e h}{p}\right)$$ (12)

Where the moment at each end of the beam, $M_e = \frac{\alpha ph^2}{12}$

Where α is the % fixity at ends of the beam, then:

$$\Delta_{max.elastic} = \frac{(5 - 4\alpha)ph^4}{384E_c I}$$ (13)

Eq. 13 ignores the small contribution of membrane retrofit to the stiffness of the wall and is therefore slightly conservative. It is easily shown that Eq. 13 yields:

$$\Delta_{max.elastic} = \frac{5ph^4}{384E_c I}$$ For simply supported beams ($\alpha = 0\%$) Checks ✔

$$\Delta_{max.elastic} = \frac{ph^4}{384E_c I}$$ For fixed end beams ($\alpha = 100\%$) Checks ✔

11

Resistance Function

Eqs. 9 and 13 are two equations and three unknowns (Δ, y, and p). Furthermore, Eq. 13 can only be used for elastic deflection of the wall. The solution may be found by examining the curvature of the wall as it undergoes bending (Priestly and Paulay 1992). At the onset of crack, the curvature at the central section of the wall (Fig. 4) is:

$$\Phi_{cr} = \frac{\sigma_{cr}}{E_c t} \tag{14}$$

And:
$$\Delta_{cr} = \frac{(5 - 4\alpha)ph^4}{384 E_c I}$$

It may conservatively be assumed that the displacement Δ increases in proportion with the central curvature. Thus, the following equation is derived for the wall curvature as crack grows:

$$\Phi_{cr} = \frac{\sigma_{crG}}{E_c (t - y)} \tag{15}$$

Also:
$$\sigma_{cr} = \frac{2R_{cr}}{t} \tag{16}$$

And:
$$\sigma_{crG} = \frac{2R_{crG}}{(t - y)} \tag{17}$$

Setting:
$$\beta = \frac{\Phi_{crG}}{\Phi_{cr}} = \frac{R_{crG} t^2}{R_{cr}(t - y)^2} \tag{18}$$

Then:
$$\Delta_{crG} = \beta \, \Delta_{cr} \tag{19}$$

The wall resistance function in terms of displacement versus lateral load can now be derived in an iterative fashion. At the onset of crack ($y = 0$), the problem is reduced to two Eqs. 9 and 13 and two unknowns (Δ and p). As crack grows ($y > 0$), Δ is calculated using Eq. 19, and "p" is subsequently calculated using Eq. 9. When this process is

programmed for small increments of y, the result is the full resistance definition of the wall through failure.

Membrane Retrofit Concrete Masonry Wall

Analytical Model

Membrane retrofit materials used for the lateral load conditions described in this paper must exhibit significant ductility for large deflections. Ease of application and low cost are important factors in selection of membrane retrofits. The membrane retrofit materials such as polymers may be sprayed on, trowled-on, or attached with adhesives to the tension face of the wall. Other membrane materials such as thin steel or aluminum sheets may be attached to the tension face of the wall using masonry screws, expansion bolts, or other structurally sound methods (Fig. 5).

The assumptions made for analytical models of the unreinforced case will stand for this case as well. Consider the wall in Fig. 6, partially fixed end conditions at top and bottom, and lateral pressure "p". The added parameter represents the membrane retrofit at the crack opening. Although the membrane retrofit covers the entire inside surface of the wall, the tributary length of the membrane affected by crack opening is far less than the height of the wall. The tributary length (l) depends on how the membrane retrofit is attached to the concrete masonry, and how far the membrane strain extends past the crack opening. The shorter the tributary length, the higher the membrane strain is due to crack opening. During blast tests conducted by Dinan et al. (2003), it was observed that the length of polyurea membrane retrofits strained on each side of the crack opening was generally equal to one half of the concrete masonry block height. The approximate

tributary length of polymer membrane retrofit is therefore assumed to be between 8 to 12 inches in this paper. More accurate estimates of the tributary length of specific polymers may be obtained by test or analysis and used in the analytical model. For membrane retrofits discretely fastened to the masonry wall, the tributary length is the vertical distance between fasteners (Fig. 5). Summing moments about the base of the wall result in:

$$\circlearrowleft + \sum M_{base} = 0 = Hh - \frac{ph^2}{2} - \frac{w_i \Delta}{2} \tag{20}$$

$$H = \frac{ph}{2} + \frac{w_i \Delta}{2h} \tag{21}$$

$$\circlearrowleft + \sum Mo = 0 = -\frac{ph^2}{8} + \frac{w_i \Delta}{4} + \left(\frac{ph}{2} + \frac{w_i \Delta}{2h} \right) \frac{h}{2} - \frac{\alpha p h^2}{12} + P\Delta - Rx - \frac{Tt}{2} \tag{22}$$

$$\Delta = \frac{Rx}{\frac{w_i}{2} + P} - \frac{(3 - 2\alpha)ph^2}{12w_i + 24P} + \frac{Tt}{w_i + 2P} \tag{23}$$

$$R = \frac{w_i}{2} + P + T \tag{24}$$

It is necessary to define a relationship between wall deflection and crack opening. This is accomplished by the simplifying assumption that the two portions of the wall on each side of the crack remain plane and without distortion. The relationship can be derived from Fig. 7 as follows:

$$\frac{\Delta}{\frac{h}{2}} = \frac{\delta}{t} \tag{25}$$

$$\delta = \frac{2t\Delta}{h} \tag{26}$$

This relationship provides the necessary tool to calculate the tension in the membrane retrofit as the crack opens.

$$f_t = \frac{E_r \delta}{\dfrac{l}{2}}$$

(27)

$$T = f_t A = f_t t_r (1) \qquad \text{per unit width of membrane retrofit}$$

(28)

$$T = \frac{4 E_r t_r t \Delta}{lh}$$

(29)

The discussions for stress distribution across the concrete masonry cross section are applicable to this case as well. As the crack grows and the membrane retrofit stretches past its yield point, the modulus of elasticity of membrane retrofit used in Eq. 29 follows the values defined in its respective stress strain curve. For example, the modulus of elasticity of polyurea used in blast tests follows the elastic-plastic behavior pattern shown in Fig. 8. Substituting Eqs. 8, 24, and 29 into Eq. 23 results in a final equation for wall displacement versus lateral load:

$$\Delta = \frac{\left(\dfrac{t}{6} + \dfrac{y}{3} - \dfrac{(3 - 2\alpha) p h^2}{12 w_i + 24 P} \right)}{1 - \left(\dfrac{4 E_r t_r t}{lh} \right)\left(\dfrac{4t + 2y}{3 w_i + 6P} \right)}$$

(30)

Resistance Function

The wall resistance function in terms of displacement versus lateral load can now be derived in an iterative fashion. At the onset of crack when $y = 0$, the problem is reduced to two Eqs. 30 and 13 and two unknowns (Δ and p). As crack grows ($y > 0$), it is assumed that Δ increases in proportion with the central curvature of the wall and is

15

calculated using Eq. 19. "*p*" is subsequently calculated using Eq. 30. When this process is programmed for small increments of "*y*", the result is the full resistance definition of the wall through failure. The resistance function is truncated when:

1. The maximum compressive stress in the CMU material exceeds *0.85f'$_m$*

2. The calculated pressure or resistance is a negative value

3. The maximum tensile or shear stresses in the membrane retrofit exceed its ultimate strength

4. The maximum shear in fasteners or adhesive bond for the membrane retrofit is exceeded

Membrane Retrofit Concrete Masonry Walls with Arching Action

Analytical Model

As the load increases, the wall is pushed against the unyielding supports creating thrust forces "V_u" at the ends (Fig. 9). A *three-hinged arch* is formed where the external moment is resisted by the internal couple "$V_u\,r_u$" where "r_u" is the height of the arch. The thrust force is a function of the material properties of the mortar joint and the contact area.

$$M_u = V_u\,r_u \tag{31}$$

Consider the wall in Fig. 10 with thrust forces at top and bottom due to arching, and membrane retrofit on the tension face of the wall. Although the membrane retrofit covers the entire inside surface of the wall, the tributary length of the membrane affected by

crack opening at mid-span is far less than the height of the wall. The tributary length (l) of the membrane retrofit is treated in the same manner as that of the previous case.

Summing moments about the base of the wall result in:

$$\circlearrowleft \sum M_B = 0 = H_{Top}h - \frac{ph^2}{2} + P\left(\frac{t-a}{2}\right) + w_i\left(\frac{t-a}{2} - \frac{\Delta}{2}\right) \tag{32}$$

$$H_{Top} = \frac{ph}{2} - (P + w_i)\left(\frac{t-a}{2h}\right) + \frac{w_i\Delta}{2h} \tag{33}$$

$$H_{Bottom} = \frac{ph}{2} + (P + w_i)\left(\frac{t-a}{2h}\right) - \frac{w_i\Delta}{2h} \tag{34}$$

Summing moments about point "O" for the top half of the wall results in:

$$\circlearrowleft + \sum Mo = 0 = P\left(\frac{t-a}{2}\right) + \left(\frac{w_i}{2}\right)\left(\frac{t-a}{2} - \frac{\Delta}{2}\right) - R\left(x + \frac{t-a}{2} - \Delta\right) - T\left(\frac{a}{2} + \Delta\right)$$

$$+ \left(\frac{ph}{2}\right)\left(\frac{h}{4}\right) \tag{35}$$

$$\Uparrow + \sum Fy = 0 = R - P - T - V_{top} - \frac{w_i}{2} \tag{36}$$

$$R = T + P + V_{top} + \frac{w_i}{2} \tag{37}$$

Stresses in the masonry are distributed in a triangular form as shown Fig. 4, and the relationship between x and y distances are shown by Eq. 8. As the crack opens, tension in the membrane retrofit is calculated using Eq. 29.

$$T = \frac{4E_r t_r t}{lh}\Delta = \Omega\Delta$$

Where: $\Omega = \dfrac{4E_r t_r t}{lh}$ (38)

As the crack grows and the membrane retrofit stretches past its yield point, the modulus of elasticity of membrane retrofit used in Eq. 38 follows the values defined in its respective stress strain curve.

McDowell et al. (1956) proposes the strain equation in the arching section of the wall:

$$\varepsilon = \dfrac{2\delta}{\dfrac{h}{2}}$$ (39)

$$\sigma = \dfrac{4E\delta}{h} = \dfrac{4E\dfrac{2\Delta t}{h}}{h} = \dfrac{8E\Delta t}{h^2}$$ (40)

$$V_{Top} = \dfrac{8E\Delta ta}{h^2} = \eta\Delta$$ (41)

Where: $\eta = \dfrac{8E_c ta}{h^2}$ (42)

The width of the arching area may be taken as the face shell thickness of the individual concrete masonry unit, or the following simplified equation proposed by Drysdale et al. (1994):

$$a = 0.1t$$ (43)

Substituting Eqs. 8, 37, 38, and 41 into Eq. 35 and simplifying:

$$0 = \eta\Delta^2 - \left(\Omega\left(\dfrac{4t+2y}{6}\right) + \eta\left(\dfrac{4t+2y-3a}{6}\right) - P - \dfrac{w_i}{4}\right)\Delta - \left(P + \dfrac{w_i}{2}\right)\left(\dfrac{t+2y}{6}\right) + \dfrac{ph^2}{8}$$ (44)

And in terms of pressure:

$$p = -\frac{8}{h^2}\left(P\left(\frac{t-a}{2}\right) + \frac{w_i}{2}\left(\frac{t-a}{2} - \frac{\Delta}{2}\right) - \left(T + P + V_{Top} + \frac{w_i}{2}\right)\left(x + \frac{t-a}{2} - \Delta\right) - T\left(\frac{a}{2} + \Delta\right)\right)$$

$$(45)$$

Before initiation of crack at $y = 0$, it is safe to assume that tension in the retrofit is zero and arching forces are also zero. Eq. 44 reduces to:

$$\left(P + \frac{w_i}{4}\right)\Delta - \left(P + \frac{w_i}{2}\right)\left(\frac{t}{6}\right) + \frac{ph^2}{8} = 0 \qquad (46)$$

Hence:

$$\Delta = \frac{\left(P + \frac{w_i}{2}\right)\left(\frac{t}{6}\right) - \frac{ph^2}{8}}{P + \frac{w_i}{4}} \qquad (47)$$

It is safe to assume that when $y = 0$, the wall exhibits elastic bending and its deflection may also be calculated from the following equation for a fixed end beam:

$$\Delta = \frac{ph^4}{384E_c I} \qquad (48)$$

Equating Eqs. 47 and 48 results in Eq. 49 from which pressure at $y = 0$ is calculated and later deflection Δ:

$$p = \frac{\left(P + \frac{w_i}{2}\right)\left(\frac{t}{6}\right)}{\left(\frac{h^4}{384E_c I}\right)\left(P + \frac{w_i}{4}\right) + \frac{h^2}{8}} \qquad (49)$$

It may conservatively be assumed that the displacement Δ increases in proportion with the central curvature. Therefore, Eq. 19 holds for this case as well. The wall resistance

function in terms of displacement versus lateral load can now be derived in an iterative fashion. At the onset of crack ($y = 0$), the problem is reduced to two Eqs. 48 and 49 and two unknowns (Δ and p). As crack grows ($y > 0$), "Δ" is calculated using Eq. 19, and "p" is subsequently calculated using Eq. 45. When this process is programmed for small increments of "y", the result is the full resistance function of the wall through failure. The resistance function is truncated for the four conditions stated for the previous case.

Effect of Windows and Doors

In common building construction, concrete masonry walls often incorporate windows and/or doors. The impact of window or door opening on the wall resistance and response to lateral pressure depends on several factors:

1. Windows and doors are designed to resist the lateral pressure experienced by the wall and stay intact: The lateral pressure on the wall remains the same, but the resistance of the wall is reduced and so is the weight of the wall. The reduction in the resistance function of the wall was examined by Mays et al. (1998) for reinforced concrete walls and by Flanagan and Bennett (1999) in the context of masonry. The factor designated by "B_w" is computed for the wall and used to reduce the resistance function of the same wall with no openings.

$$B_w = \frac{A_{OP}}{A_{Surface}} \qquad (50)$$

Where:

A_{OP} = Solid surface area of wall with openings

$A_{Surface}$ = Solid surface of wall with no openings

2. Windows and doors are not designed to resist the lateral pressure experienced by the wall, and are blown out of place or destroyed leaving an opening: The lateral pressure on the wall, the mass of the wall, and the resistance function of the wall are reduced. The reduction in the resistance function of the wall is calculated using Eq. 50. The reduction in lateral pressure as well as the reduction in the weight of the wall may be approximated by using the same equation.

Wind Capacity

A 113 kph wind is associated with 0.6 kPa of pressure on the surface of a building. Wind pressure is proportional to the square root of wind speed. Therefore, a simple relationship as shown in Eq. 51 will allow for the computation of wall wind capacity in terms of wind speed (kph) when the wall pressure capacity is calculated using the methodology set forth herein.

$$\text{Wall Wind Capacity} = 113\sqrt{\frac{p}{0.6}} = 146\sqrt{p} \ \text{kph} \tag{51}$$

Where: p = Maximum pressure capacity of the wall (kPa)

Example

This is shown using the following example for a top and bottom simply supported CMU wall:

$h = 3.67$ m $t = 194$ mm $w_i = 6.83$ N per mm of wall width

$P = 0.0$ lb N per mm of wall width $I = 4.65 \times 10^5$ mm^4 per mm of wall width

$E_c = 13.8 \times 10^6$ kPa $t_r = 0.0$ or 3.0 mm

$f'_m = 13,780$ kPa CMU ultimate compressive strength $E_r = 234,260$ kPa

$l = 305$ mm tributary length of retrofit $F_t = 11,713$ kPa retrofit tensile strength

Calculations show that the unreinforced CMU wall withstands up to 63 kph wind. It is noted that the wind resistance of this wall is far below the current design value of 113-129 kph because tension is not allowed in the wall. For the same wall with 3 mm polymer retrofit the wind capacity is 300 kph, and for the same wall with arching action and 3 mm polymer the wind capacity is increased even more.

CMU Material Properties

Weight = 142.4 N   Volume = 6.014×10^6 mm^3

Mass Density = 0.00242 g/mm^3

Ultimate Compressive Strength (f'_m) = 13,780 kPa

$E = 13.8 \times 10^6$ kPa   *Poisson's ratio* = 0.15 to 0.2 $G = 5.742 \times 10^6$ kPa

Ultimate Tensile Strength = $\dfrac{1}{10} f'_c = 1,378 - 1,732$ kPa

Ultimate Shear Strength = 689 kPa   Mortar $f'_c = 12,400 - 17,220$ kPa

Mortar Tensile Strength = 1,550 kPa

Mortar Tensile Bond Strength = $345 - 1,034$ kPa

The modulus of elasticity calculated based on the following equation:

$E_c = (750 \text{ to } 1000) \times f'_m = 10.335 \times 10^6 \text{ to } 13.8 \times 10^6$ kPa

Analysis Results and Discussions

For both wall models, tensile stresses are not allowed to develop in the concrete masonry part of the wall. In the first model, it is shown that the presence of membrane retrofit greatly enhances the resistance function of the unreinforced wall (Figs. 11 thru 14). The peak resistance of the unreinforced concrete masonry wall is shown in Fig. 11 at 0.19 kPa

compared to 8.3 kPa for the same wall with 6 mm thick polyurea retrofit. The stronger retrofit materials such as steel and aluminum increase the wall resistance significantly to 23 kPa for 0.8 mm thick steel and 15.5 kPa for 0.8 mm thick aluminum.

In the second model where arching is considered, the peak resistance of unreinforced concrete masonry wall to lateral pressure improves to 42 kPa as shown in Fig. 15. When membrane retrofits are considered for this model, the improvement in the resistance function depends on the type of membrane retrofit. For polyurea, the improvement is not significant where the peak resistance increases to 43 kPa for 3 mm thick polyurea and 44 kPa for 6 mm thick polyurea (Fig. 16). Membrane retrofit materials with better structural properties make noticeable improvement in the wall resistance function. The peak resistance improves to 55 kPa for 0.5 mm thick steel and 64 kPa for 0.8 mm thick steel (Fig. 17). The peak resistance improves to 50 kPa for 0.5 mm thick aluminum and 57 kPa for 0.8 mm thick aluminum (Fig. 18).

In general, the presence of membrane retrofit results in the tension force T (Figs. 6 and 10) and allows the wall to deflect beyond the wall thickness without upsetting its equilibrium.

Conclusions and Recommendations

This paper provides the formulation for the resistance of membrane retrofit concrete masonry walls to lateral uniform pressure. Resistance functions are provided for two separate cases:

1. Unreinforced concrete masonry walls with and without membrane retrofit

2. Unreinforced concrete masonry walls with and without membrane retrofit, and with arching action

The results may be used in high risk areas to enhance the construction of new buildings using unreinforced concrete masonry walls, as well as to retrofit similar walls in existing buildings or homes. For arching action to develop, care must be taken to ensure gaps are not present between the wall and its top and bottom interfaces. Although membrane retrofit concrete masonry walls have shown great results in seismic and blast tests, further studies are recommended to quantify the improvement of this system for wind conditions as well as verification of the analysis results by test. The studies should concentrate on:

a. The application of polymer retrofit materials to concrete masonry walls: To date, there is no objective evidence that polyurea or similar polymer retrofits lack adequate adherence to the surface of concrete masonry. However, little research has been performed to accurately determine the adherence of polymers to concrete masonry surfaces.

b. Application of the membrane retrofit material to the bottom and top boundaries of the wall needs to be investigated. Adequate extension and attachment of the membrane retrofit through the top and bottom supports play a major role in the structural integrity of the wall system.

c. Wind tunnel tests of full-size or reduced-size membrane retrofit walls will allow for better instrumentation of the wall and membrane retrofit. The results will be used to fine-tune the current analytical models.

d. Static and dynamic tests to better define the strain for the arching ends: To date, little is published in the literature on the behavior of the arching ends of the wall system. Knowledge of crushing behavior of the arched end while the wall experiences large deflections is important to the accuracy of the current analytical models.

Acknowledgement

REFERENCES

Baker L.R. (1977), "The Failure Criterion of Brickwork in Vertical Flexure," *in Proceedings of the Sixth International Symposium on Loadbearing Brickwork*, London, England, PP. 203-216.

Baker, L.R. (1980), "Lateral Loading of Masonry Panels: Structural Design of Masonry," *Cement and Concrete Association of Australia*, Sydney, Australia.

Davidson, J.S., Porter, J.R., Dinan, R.J., Hammons, M.I., Connell, J.D. (May 2004). "Explosive Testing of Polymer Retrofit Masonry Walls." *Journal of Performance of Constructed Facilities*, ASCE, Vol. 18, No. 2, 100-106.

Davidson, J.S., Fisher, J.W., Hammons, M.I., Porter, J.R., Dinan, R.J. (August 2005). "Failure Mechanisms of Polymer-Reinforced Concrete Masonry Walls Subjected to Blast." *Journal of Structural Engineering*, ASCE, Vol. 131, No. 8, 1-12.

Dennis, S. T. (1999). "*Masonry walls subjected to blast loading-DYNA3D analysis.*" U.S. Army Engineer Waterways Experiment Station, Vicksburg, Mississippi.

Dennis, S. T., Baylot, J. T., and Woodson, S. C. (2000). "Response of ¼ scale concrete masonry unit (CMU) walls to blast." *Proc., ASME Pressure Vessels and Piping Conference*, Seattle, Washington.

Dinan, R.J., Fisher, J.W., Hammons, M.I., Porter, J.R. (2003). " Failure mechanisms in unreinforced concrete masonry walls retrofitted with polymer coatings," *Proceedings of the 11th international Symposium on Interaction of the Effects of Munitions with Structures*, May 5-9, 2003.

Drysdale, R.G., Hamid, A.A., Baker, L.R. (1994). *Masonry and Structures: Behavior and Design*, Prentice Hall, Englewood Cliffs, New Jersey 07632.

Drysdale, R. G., Hamid A. A., and Baker L. R. (1999). *Masonry structures: behavior and design*. The Masonry Society, Boulder, Colorado.

Engineering Technical Letter (ETL) 02-4: *Airblast Protection Polymer Retrofit of Unreinforced Concrete Masonry Walls*, Department of the Air Force, Tyndall AFB, FL.

Fattal, S. G. and Cattaneo, L. E. (1976). "Structural Performance of Masonry Walls Under Compression and Flexure", National Bureau of Standards, *Building Science Series*, No. 73.

Flanagan, Roger D., and Bennett, Richard M (1999). "Arching of Masonry Infilled Frames: Comparison of Analytical Methods." *Pract. Per. Struct. Des. Constr.*, 4(3), 105-110.

Gabrielsen, B. L., Wilton, C. (1973). *"Shock Tunnel Tests of Preloaded and Arched Wall Panels"*, Report #AD-764 263 prepared for the Defense Civil Preparedness Agency, URS Research Company, Distributed by National Technical Information Service, US Department of Commerce, Springfield, VA, U.S.A.

Gabrielsen, B. L., Wilton, C., Kaplan, K. (1975). *"Response of Arching Walls and Debris from Interior Walls Caused by Blast Loading"*, Final Report prepared for the Defense Civil Preparedness Agency, Scientific Services, Inc., Redwood City, CA, U.S.A.

Hamid, A.A. and Drysdale, R.G. (January 1988). "Flexural tensile strength of concrete block masonry." Technical Paper, *Journal of Structural Engineering*, Vol. 114, No.1. pp. 50-66.

Kariotis, J.C., Ewing, R.D., and Johnson, A.W. (1985), "Predictions of Stability for Unreinforced Brick Masonry Walls Shaken by Earthquakes", *Proc. 7th Internationals Brick Masonry Conference*, Melbourne, 2: 1175-1184.

Kariotis, J.C., Ewing, R.D., Johnson, A.W., and Adham, S.A. (1985), "Methodology for Mitigation of Earthquake Hazards in Unreinforced Brick Masonry Buildings", *Proc. 7th Internationals Brick Masonry Conference*, Melbourne, 2: 1339-1350.

Knox, K. J., Hammons, M. I., Lewis, T. T., and Porter, J. R. (2000). *"Polymer materials for structural retrofit."* Force Protection Branch, Air Expeditionary Forces Technology Division, Air Force Research Laboratory, Tyndall AFB, Florida.

La Mendola, L.L., Papia, M., Zingone, G. (1995), "Stability of Masonry Walls Subjected to Seismic Transverse Forces", *Journal of Structural Engineering*, ASCE, Vol. 121 (11), 1581-1587.

Laursen, P. T., Seible, F., and Hegemeir, G. A. (1995). "Seismic retrofit and repair of reinforced concrete with carbon overlays." *Rep. No. SSRP-95/01*, Structural Systems Research Project, University of California, San Diego, California.

Martini, K. (1996). "Research in the out-of-plane behavior of unreinforced masonry." Ancient Reconstruction of the Pompeii Forum, School of Architecture, University of Virginia, Charlottesville, Virginia, USA.

Martini, K. (1996b), "Finite element studies in the two-way out-of-plane behavior of unreinforced", masonry, Ancient Reconstruction of the Pompeii Forum, School of Architecture, University of Virginia, Charlottesville, Virginia, USA.

Martini, K. (1997), "Research in the Out-of-Plane Behavior of Unreinforced Masonry", Department of Architecture and Civil Engineering, University of Virginia, Charlottesville, Virginia, USA.

Mays, G.C., Hetherington, J.G., and Rose, T.A. (1998). "Resistance-Deflection Functions for Concrete Wall Panels with Openings." *J. Struct. Eng.*, 124(5), 579-587.

McDowell, E.L., McKee, K.E., ASCE, A.M., Sevin, E. (1956), "Arching Action Theory of Masonry Walls", Journal of Structural Division, *Proceedings of ASCE*, ST 2, Paper 915, PP 1-18.

Paulay, T. and Priestley, M.J.N. (1992), *"Seismic Design of Reinforced Concrete and Masonry Buildings*, J. Wiley, New York.

Priestley, M.J.N. (1985), "Seismic Behaviour of Unreinforced Masonry Walls", *Bulletin of the New Zealand National Society for Earthquake Engineering*, Vol. 18, No. 2, PP 191-205.

Priestley, M.J.N.; Robinson, L.M. (1986), "Discussion: Seismic Behaviour of Unreinforced Masonry Walls", *Bulletin of the New Zealand National Society for Earthquake Engineering*, Vol. 19, No. 1, PP 65-75.

Tropical Report 08, ABK Consultants (1984), *"Methodology for Mitigation of Seismic Hazards in Existing Unreinforced Masonry Buildings"*, El Segundo, CA.

Yokel, F. Y. (1971). "Stability and Load Capacity of Members with no Tensile Strength"

  Proc., American Society of Civil Engineers, Journal of the Structural Division, ST 7,

  1913 – 1926.

Yokel, F. Y., and Dikkers, R. D. (1971). "Strength of load bearing masonry walls." *Proc.,*

  American Society of Civil Engineers, Journal of the Structural Division, 97, 1593 –

  1609.

LIST OF ACRONYMS

AFB	Air Force Base
AFRL	Air Force Research Laboratory
CMU	Concrete Masonry Unit
DOD	Department Of Defense
FE	Finite Element
g	gram
kPa	kiloPascal
kph	kilometer per hour
m	meter
mm	millimeter
N	Newton
S.S.	Simply Supported
UAB	University of Alabama at Birmingham
WAC	Wall Analysis Code

LIST OF NOTATIONS

A_{op}	Solid surface area of wall with openings
$A_{Surface}$	Solid surface of wall with no openings
B_w	Area ratio
c	Radius of curvature
E	Elastic modulus
E_c	Concrete masonry elastic modulus
E_r	Membrane retrofit elastic modulus
f_c	Compressive stress
f_{cr}	Compressive stress at the onset of crack
f'_m	Concrete masonry compressive strength
ε_{cu}	Ultimate strain
H	Horizontal reaction force
h	Height of wall, inch
I	Concrete masonry wall moment of inertia
l	Tributary length of membrane retrofit
M	Moment
M_{cr}	Moment at the onset of crack
m	Mass
p	Lateral pressure
P	Wall surcharge
R	Resultant force of the compressive stresses in the wall
R_{cr}	Resultant force of the compressive stresses in the wall at the onset of crack

R_{crG}	Resultant force of the compressive stresses in the wall as crack grows
σ_{cr}	Bending stress in the concrete masonry at the onset of crack
σ_{crG}	Bending stress in the concrete masonry as crack grows
t	Wall thickness
t_r	Membrane retrofit thickness
T	Tension in the membrane retrofit
x	Distance from R to the wall centerline
y	Crack length
w_i	Wall weight
α	Wall end fixity, %
β	Wall curvature ratio
Δ	Wall lateral displacement
Δ_{cr}	Wall lateral displacement at the onset of crack
Δ_{crG}	Wall lateral displacement as crack grows
Φ	Curvature of central section of wall
Φ_{cr}	Curvature of central section of wall at the onset of crack
Ω	Factor used for tension in the membrane retrofit
η	Factor used for arching force

LIST OF FIGURES

LIST OF TABLES

Fig. 1. Unreinforced masonry wall spanning vertically and subjected to lateral load
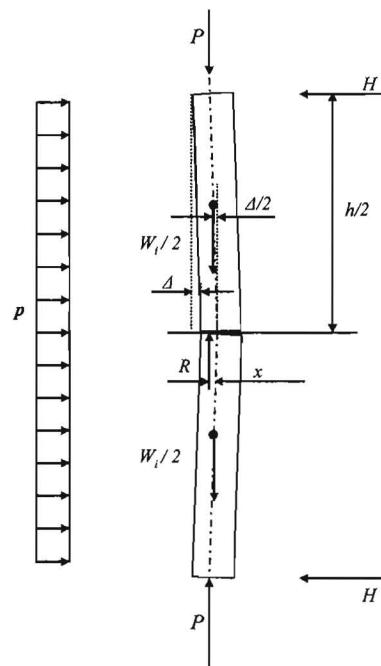
Fig. 2. Moment equilibrium for face-loaded wall
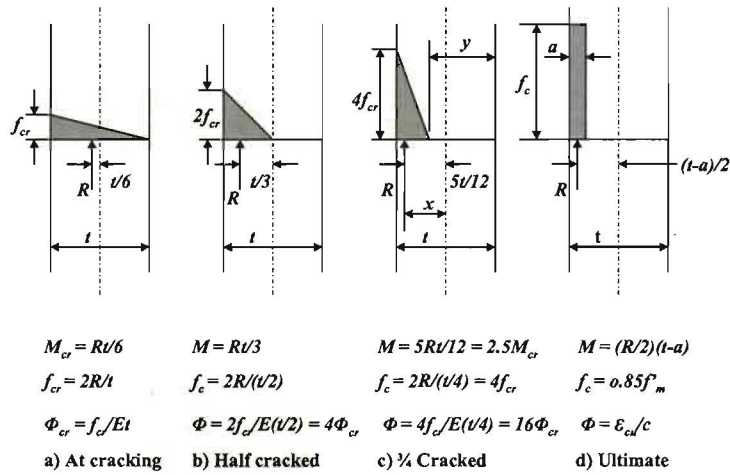
37
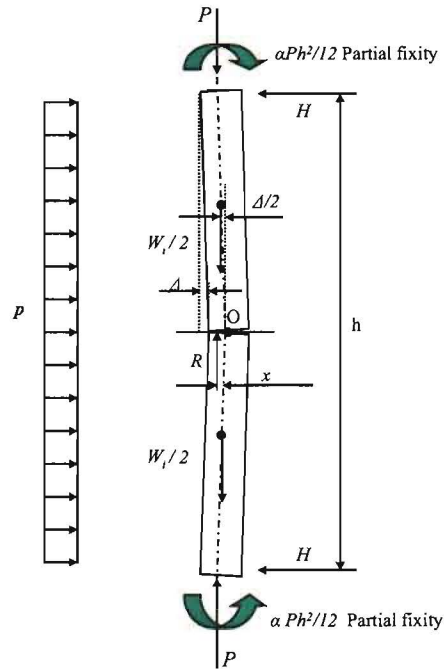
Fig. 3. Free-body diagram of wall

$M_{cr} = Rt/6$	$M = Rt/3$	$M = 5Rt/12 = 2.5M_{cr}$	$M = (R/2)(t-a)$
$f_{cr} = 2R/t$	$f_c = 2R/(t/2)$	$f_c = 2R/(t/4) = 4f_{cr}$	$f_c = 0.85f'_m$
$\Phi_{cr} = f_{cr}/Et$	$\Phi = 2f_c/E(t/2) = 4\Phi_{cr}$	$\Phi = 4f_c/E(t/4) = 16\Phi_{cr}$	$\Phi = \varepsilon_{cu}/c$
a) At cracking	b) Half cracked	c) ¾ Cracked	d) Ultimate

Fig. 4. Stress distribution

Fig. 5. Metal sheet retrofit configuration

Fig. 6. Free-body diagram of membrane retrofit concrete masonry wall
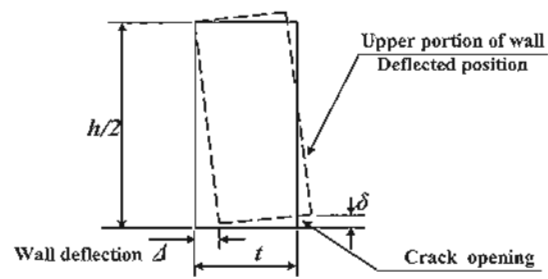
Fig. 7. Wall deflection versus crack opening
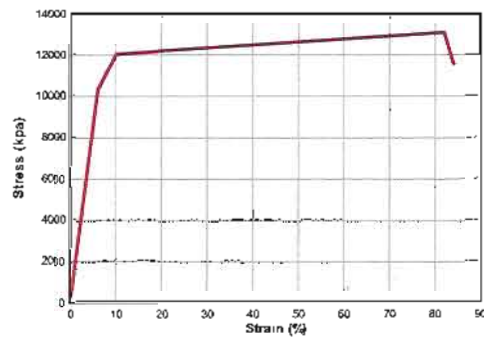
Fig. 8. Static Stress-Strain Curve for the Spray-On Polymer
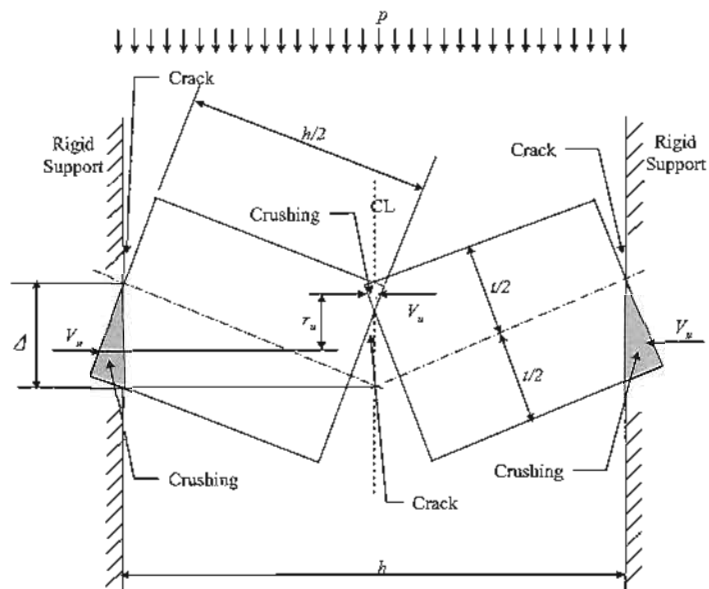
Fig. 9. Wall with arching action in a deflected position
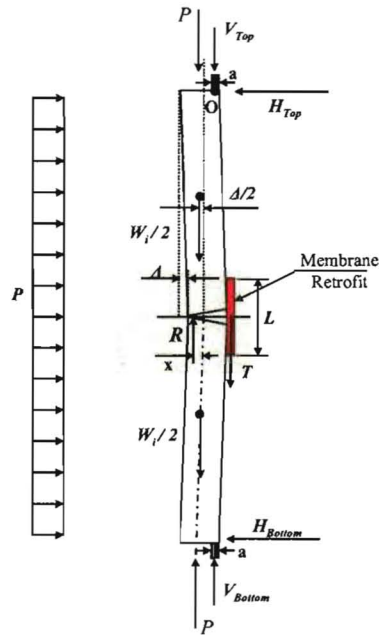
Fig. 10. Free-body diagram of membrane retrofit wall with arching action
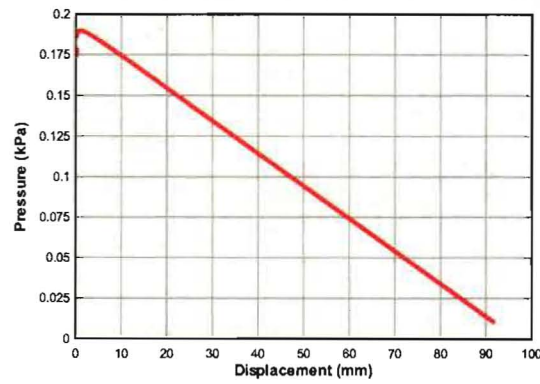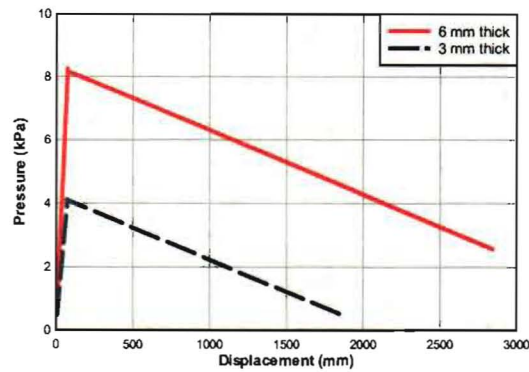

Fig. 11. Resistance Function – unreinforced CMU wall
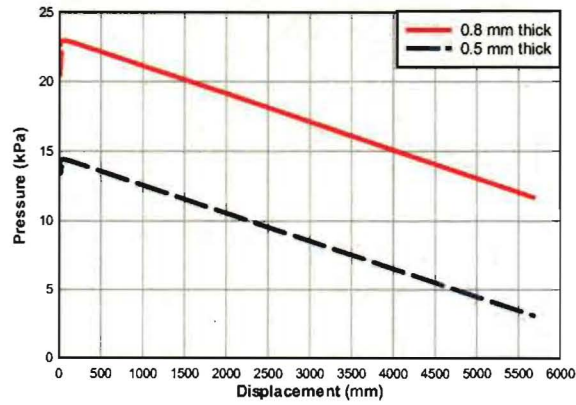

Fig. 12. Resistance Function – polyurea retrofit

41

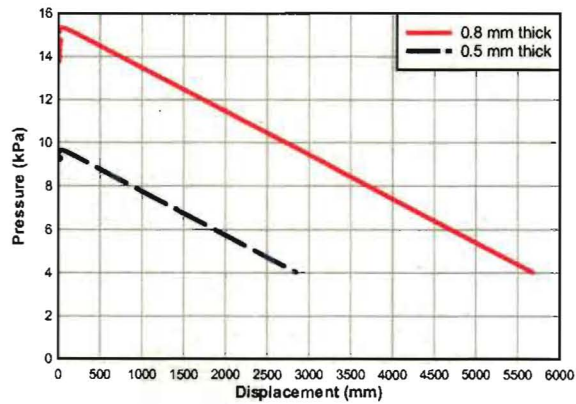Fig. 13. Resistance Function – steel sheet retrofit

Fig. 14. Resistance Function – aluminum sheet retrofit

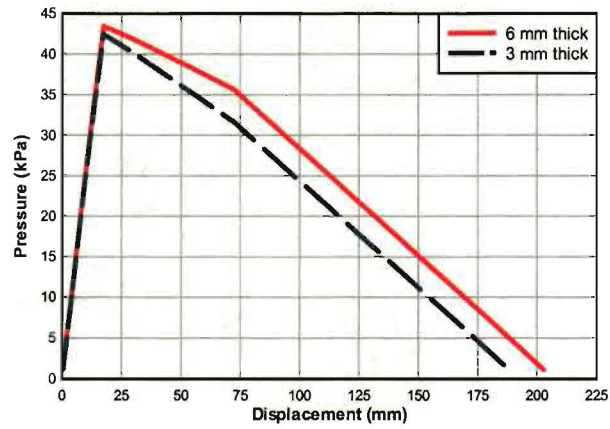Fig. 15. Arching Resistance – unreinforced CMU wall

42
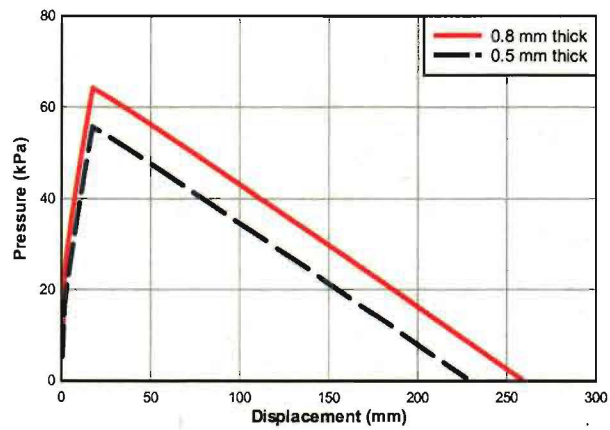
Fig. 16. Arching Resistance – polyurea retrofit
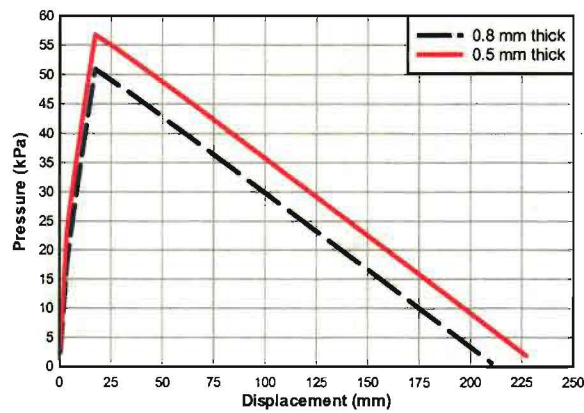

Fig. 17. Arching Resistance – steel sheet retrofit

Fig. 18. Arching Resistance – aluminum sheet retrofit

TABLE 1. Properties of Polyurea

Property	Value
Modulus of Elasticity	234,260 kPa
Tangent Modulus	23,426 kPa
Elongation at Rupture	89%
Stress at Rupture	13,856 kPa
Maximum Tensile Strength	14,050 kPa
Density	14,304 N/m^3
Poisson's Ratio	0.4
Shear Modulus	80,062 kPa